Journal Name

RSCPublishing

ARTICLE

Functionalized layered double hydroxide-based epoxy nanocomposites with improved flame retardancy and mechanical properties

Cite this: DOI: 10.1039/x0xx00000x

Received 00th December 2014,
Accepted 00th January 2014

DOI: 10.1039/x0xx00000x

www.rsc.org/

Ehsan Naderi Kalali,[a] Xin Wang, [a] De-Yi Wang*[a]

Abstract: Functionalized layered double hydroxides (LDHs) based on multi-modifiers' system composed by hydroxypropyl-sulfobutyl-beta-cyclodextrin sodium (sCD), dodecylbenzenesulfonate (DBS) and taurine (T) were designed and fabricated in this paper, aiming at developing high performance fire retardant epoxy nanocomposites. In this multi-modifiers' system, sCD was utilized to improve the char yield, DBS was used to enlarge the inter-layer distance of LDH and T was used to enhance the interaction between epoxy matrix and LDH layers. Based on these functionalized LDHs, bisphenol A epoxy resin and diamino diphenyl sulfone (DDS), series functionalized LDH/Epoxy nanocomposites have been developed. The structural morphology of LDH/epoxy nanocomposites was investigated by transmission electron microscopy (TEM) and wide-angle X-ray scattering (WAXS), revealing that sCD-DBS-T-LDH/EP showed much better dispersion state than the epoxy composites containing un-modified LDH or single modifier modified LDH. Importantly, with only 6 wt% functionalized LDH, sCD-DBS-T-LDH/EP nanocomposite reached V0 rating in UL-94 vertical burning testing. Furthermore, the incorporation of sCD-DBS-T-LDH into epoxy led to a significant reduction in peak heat release rate, total heat release and total smoke production, which exhibited superior fire resistance over its counterparts at the equivalent filler loading. The notably improved fire resistance could attribute to the formation of the consolidated and compact char layers during combustion which significantly suppressed heat and mass transfer between polymer matrix and flame zone. Additionally, sCD-DBS-T-LDH/EP showed best impact and tensile strengths than those of other LDH/epoxy composites. This work had been offering a new approach to develop high performance fire retardant polymer/LDH nanocomposites.

1. Introduction

As one of the most important thermosetting polymers, epoxy resin (EP) has acquired wide application in the fields of coating, adhesive, electronic/electrical insulation, and laminates and composites [1-3]. EP possesses many outstanding advantages, such as low shrinkage, high thermal and mechanical stabilities and excellent solvent and chemical resistance [4-6]. However, like most of polymeric materials, EP has a fatal drawback of high flammability, which has severely restricted the application fields required a remarkable flame-retardant grade. Therefore, to improve the fire resistance of EP has motivated many researchers' interests in the worldwide range.

Over the past few decades, various phosphorus- [7, 8], silicon- [9-11], boron-containing [12] compounds have been incorporated into epoxy resins to improve the flame retardancy. Although a high level fire resistance has been achieved, a major problem encountered with these compounds was the high loading required. The arising of nanocomposite technology has provided a revolutionary new solution to flame retardant polymer materials

and it was reported that a significant improvement on the fire retardancy had been achieved by introducing a low loading of nano-fillers [13, 14]. In recent years, layered double hydroxides (LDHs), as a new fascinating nano-filler, have been widely investigated in polymer composites [15-18]. The chemical formula of LDH can be represented by $[M^{2+}{}_{1-x}M^{3+}{}_{x}(OH)_2]^{x+}.[(A^{n-})_{x/n}\cdot yH_2O]^{x-}$, where M^{2+}, M^{3+}, and A^{n-} are divalent metal cations, trivalent metal cations, and interlayer anions, respectively.[19] The composition of LDHs is highly tunable due to the versatility in the species of M^{2+}, M^{3+}, and A^{n-} together with the value of "x". LDHs can also be used as flame retardant additives because of its endothermic decomposition upon exposure to high temperatures [20]. In order to facilitate the dispersion of LDHs in the polymers, it is necessary to modify the pristine LDH to enlarge the interlayer space. A wide variety of anionic surfactants, such as fatty acid salts, [21] sulfonates, [22, 23] and phosphates, [24, 25] have been used as modifiers for LDHs. In our recent study, cyclodextrin (CD)-based (Scheme 1) derivatives have been used as modifier for LDH, showing a considerable decrease in flammability properties compared with conventional modified LDH. [26] However, the interlayer distance of CD modified LDH is not large enough to facilitate the fabrication of modified LDH/polymer nanocomposites. Therefore, further functionalization for LDH would be necessary in order to obtain functionalized LDH-based polymer nanocomposites with satisfactory fire resistance and mechanical properties simultaneously.

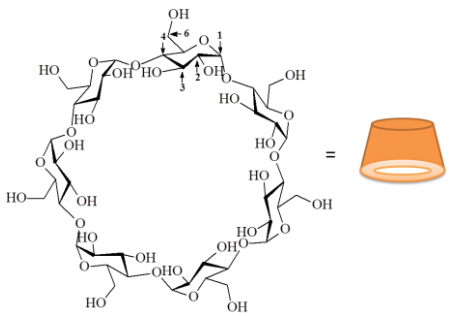

Scheme 1: The structure of β-cyclodextrin (BS)

In this work, hydroxypropyl-sulfobutyl-beta-cyclodextrin sodium (sCD) was synthesized as a first modifier for LDH since sCD contains glucopyranose units possessing large number of hydroxyl group that may lead to the formation of rich char residues; sodium dodecylbenzenesulfonate (SDBS) was used as a second co-modifier to further enlarge the interlayer distance of LDH to reach a better dispersion state in polymer matrix; meanwhile, taurine (T) was used as third co-modifier for LDH that acted as a bio-based cross-linking agent to improve the interaction between functionalized LDH and epoxy resin. Functionalized LDHs were synthesized and characterized by scanning electron microscopy (SEM), wide angle X-ray scattering (WAXS) and thermogravimetric analysis (TGA). Afterwards, these functionalized LDHs were introduced into epoxy resins to prepare series flame retardant epoxy composites. The morphology, thermal stability, flame retardant and mechanical properties of these composites were investigated systemically.

2. Experimental

2.1 Materials

$Mg(NO_3)_2\cdot 6H_2O$, $Al(NO_3)_3\cdot 9H_2O$, sodium hydroxide, SDBS, taurine, β-cyclodextrin, and 1, 4-butane sultone (BS) were purchased from Sigma-Aldrich Chemical Co. and used without further purification. Epoxy resin (Epoxydhedraz C) was supplied by R&G Faserverbundwerkstoffe GmbH- Germany. Diamino diphenyl sulfone (DDS) was provided by TCI Chemicals Company. Spectra/Por®6 dialysis membrane with MWCO 1000 was provided from Carl Roth GmbH & Co. KG, Karlsruhe, Germany.

2.2 Synthesis of hydroxypropyl-sulfobutyl-beta-cyclodextrin (sCD) [27]

In a three-neck round flask equipped with iso-barically funnel, reflux-condenser, and thermometer, β-cyclodextrin (0.02 mol), sodium hydroxide (0.11 mol) and de-ionized water (45 ml) were introduced and stirred to dissolve completely. The solution was heated to 75 °C, and then 1,4-butane sultone (0.08 mol) was added drop wise within 3 hours. The solution kept stirring for another 4 hours and then cooled down to the room temperature. pH value was adjusted to neutral with hydrochloric acid, and the by-products were removed by filtrate dialysis. After filtrate dialysis, the white-like solid product (sCD) was obtained using rotary evaporation method. The sCD could be represented by the chemical formula of $C_{42}H_{70}O_{35}\cdot(C_4H_8O_3S)_x$, where X is the substitution number of 1,4-butane sultone. On the basis of NMR (^{1}H-NMR, 500 MHz, DMSO, d, ppm): 4.82 (m, 2H), 1.63-2.21 (m, 4H)) and elemental analysis data (N:1.37%, C:35.5%, S:9.15% and H:7.27%), the degree of substitution of 1,4-butane was approximately 6, which means 6 sulfobutyl groups (s) have been covalently attached to CD.

2.3 Fabrication of functionalized LDHs

In a 1000 ml three-neck round flask equipped with iso-barically funnel, reflux-condenser and pH meter, SDBS (0.05 mol), sCD (0.025 mol), taurine (0.025 mol) and de-ionized water (300 ml) were charged and stirred until completely dissolved. Subsequently, an aqueous solution containing $Mg(NO_3)_2\cdot 6H_2O$ (0.2 mol) and $Al(NO_3)_3\cdot 9H_2O$ (0.1 mol) in de-ionized water (300 ml) was slowly added to the flask. During the synthesis process, the pH value was kept at 10 ± 0.5 by adding a 1 M NaOH aqueous solution

The resulting slurry was continuously stirred for 30 min; afterward, it was allowed to age at 75 °C for 18 h. Finally, the resulting product was filtered and washed thoroughly with de-ionized water until the pH = 7. The filtrated cake was then dried in an oven at 80 °C until a constant weight was achieved, which was called sCD-DBS-T-LDH. In addition, unmodified LDH (NO_3-LDH), T-LDH and sCD- LDH were synthesized using the same method. The synthesized routes are shown in scheme 2.

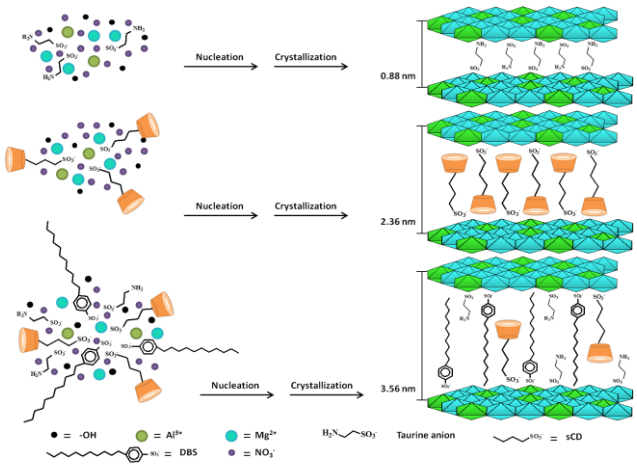

Scheme 2: Schematic diagram of anions structure intercalated in the functionalized LDH by one-step synthesis method.

2.4 Preparation of LDH/epoxy nanocomposites

A fixed weight fraction (6 wt%) of unmodified LDH (NO_3-LDH) and functionalized LDH (T-LDH, sCD-LDH and sCD-DBS-T-LDH) was used for the preparation of LDH/epoxy nanocomposites. In order to achieve a satisfactory dispersion state, two-step mixing method was applied. Firstly, LDH or functionalized LDH was incorporated into the epoxy matrix using a three-roll mill (EXAKT 80E, Germany) for 30 min; secondly, the mixture was dissolved in acetone and exposed to ultra-sonication for 20 min at 60 °C, and then acetone was removed by vacuuming at 110 °C to obtain a viscous mixture. The mixture was then heated to 180 °C in order to complete the chemical reaction between taurine and epoxy chains. Subsequently, the mixture was cooled down to 120 °C followed by adding DDS to the above mixture and stirring for 15 min until DDS totally dissolved. In order to remove the bubbles, the mixture was placed into the vacuum oven at 115 °C for 5 minutes and then immediately poured into the pre-heated PTFE moulds. The curing procedure was set as 150 °C for 1 hour, 180 °C for 2 hours and 200 °C for 2 hours. Following this procedure, NO_3-LDH/EP, sCD-LDH/EP, T-LDH/EP and sCD-DBS-T-LDH/EP were prepared respectively.

2.5 Characterization

The WAXS patterns of the samples were recorded by a XPERT-PRO X-ray diffractometer. The Cu K_α (λ = 0.1542 nm) radiation source was operated at 45 KV and 40 mA with a scan speed of 2° min^{-1}.

SEM micrographs (Nova NanoSem 230 FEG, Netherland) of nano-particles were performed to characterize the structures of LDHs before and after the modification. SEM was performed on the surface and cross-section of char residues after cone calorimeter using a Zeiss, EVO MA15 (Germany) scanning electron microscopy. All the samples were sputter-coated in gold prior to the observation.

Nanocomposite specimens with nominal dimension of 60 mm ×10 mm ×2 mm were mechanically tested under two points bending mode by a DMA Q800 Dynamic Mechanical Analyzer (TA Instruments), with an amplitude range of 30 μm and frequency of 1 Hz. The samples were heated from room temperature to 300 °C at a linear rate of 3°C/min.

TEM (Tecnai T20, FEI Company) analysis gave high magnification and detailed vision of the morphology and microstructures of the composites. Samples were prepared with a Leica ultramicrotome at room temperature. Ultramicrotomy ultrathin sections had a thickness of 50 nm. 1% uranyl acetate was added as a contrast agent. TEM analysis was carried out in a Tecnai T20 (FEI company) at 200 kV in Bright Field imaging mode.

The cone calorimeter tests were carried out on a cone calorimeter (FTT, UK) by following ISO 5660-1. The squared specimens (100 mm × 100 mm × 4 mm) were wrapped with aluminium foil and placed in a frame without grid. The specimens irradiated at a heat flux of 50 kW/m^2, corresponding to a medium fire scenario. Each sample had been tested at least 2 times.

Thermogravimetric analysis (TGA) was carried out using a Q50 (TA Instruments) thermo-analyzer instrument at a linear heating rate of 10 °C/min under a nitrogen flow and the samples were pre-heated at 160 °C under the vacuum condition prior to TGA measurement. The theoretical TG curve was computed by linear combination between the TG curves of neat EP and LDH. The formula is as follows: $W_{th}(T)_{LDH/EP} = x \times W_{exp}(T)_{EP} + y \times W_{exp}(T)_{LDH}, x + y = 1$ where, $W_{exp}(T)_{EP}$: experimental TG curve of the pure EP; $W_{exp}(T)_{LDH}$: experimental TG curve of LDH; x and y are the weight percentages of the EP and LDH in the composites, respectively.

The tensile test samples were dumbbell-shaped with dimensions of 75 mm×10 mm×2 mm, complying with ISO 527-2 (1996) standard. An Instron 5966 (USA), universal tensile testing machine equipped with a digital image correlation (DIC) system, was utilised to carry out the tensile tests a 1 mm/min test speed was used.

The Charpy impact tests of the un-notched specimens were conducted, employing a Zorn Standal Instrumented Charpy Impact Tester (Germany) at an impact speed of 2.93 m/s. The geometry of the Charpy impact test samples was rectangular with dimensions of 50 mm×6 mm×4 mm, conforming to the DIN 53753 standard.

3 Results and discussions

3.1 Characterization of functionalized LDH

The WAXS patterns of NO_3-LDH, and modified LDHs were shown in Fig. 1. In the WAXS pattern of NO_3-LDH, the first basal reflection (003) appeared at 2θ = 9.91° corresponding to an interlayer distance of 0.88 nm. For sCD-LDH, the (003) reflection shifted to 2θ = 3.75°, indicating interlayer distance of 2.36 nm. By Combination of three modifiers, DBS, sCD and T

for modification of LDH, (003) reflection shifted to the lower angle, corresponding to an interlayer distance of 3.56 nm, which was 4-fold increase in the interlayer distance compared with that of NO_3-LDH. The enlargement of the interlayer distance was caused by the relatively long molecular chains of the sCD and DBS. DBS was relatively larger (more than 2 nm) compared to the size of NO_3^- (around 0.1 nm) [19]. In contrast, incorporating taurine showed almost no change in the interlayer distance due to its small molecular size.

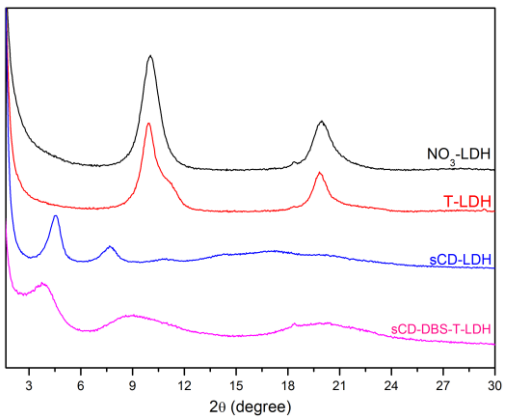

Figure 1. WAXS patterns of NO_3-LDH, T-LDH, sCD-LDH and sCD-DBS-T-LDH

Fig. 2 showed the SEM micrographs of the morphological structure of the NO_3-LDH and modified LDHs. NO_3-LDH (Fig. 2a) had a plate-like geometry of its primary particles with a microscopically smooth surface. The existence of sharp edges in most of the particles might be an indication of the incomplete process of crystal growth, resulting in no particular particle shape. The morphological features of the functionalized LDHs (Fig. 2b-2d) were similar to the NO_3-LDH and still kept the typically layered structure, meaning that the intercalation of anions did not change the two-dimensional morphology of LDH.

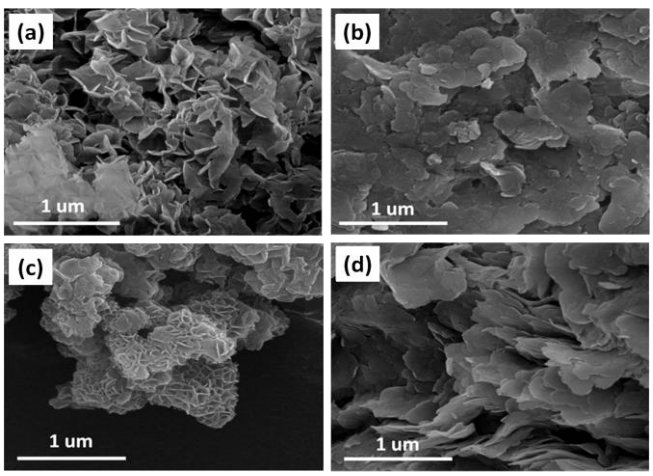

Figure 2. SEM images of (a) NO_3-LDH, (b) sCD-LDH, (c) T-LDH, and (d) sCD-DBS-T-LDH.

3.2 Structural characterization of LDH/EP nanocomposites

Usually, the structural morphology of layered nano-filler/polymer nanocomposite was characterized by X-ray scattering patterns in order to determine the microstructures. Fig. 3 showed the WAXS patterns of pure epoxy matrix, NO_3-LDH/EP, T-LDH/EP, sCD-LDH/EP and sCD-DBS-T-LDH/EP composites. Pure EP had a broad and weak diffraction peak at a 2θ value of 17.3°, due to the amorphous phase of epoxy. NO_3-LDH/EP composite showed an intense diffraction peak at a 2θ=10.1° corresponding to an inter-gallery spacing of 0.88 nm, indicating the presence of the ordered structure of unmodified LDH in the polymer matrix. T-LDH/EP exhibited a similar WAXS profile to NO_3-LDH/EP. As discussed aforementioned, the inter-gallery spaces of NO_3-LDH and T-LDH were not large enough to allow the diffusion of the resin/curing agent mixture into the inter-layers. For sCD-LDH/EP composite, a weak diffraction peak at a 2θ=3.8° was observed corresponding to an inter-gallery spacing of 2.32 nm, suggesting the swelling of LDH platelets upon polymerization. In the case of sCD-DBS-T-LDH/EP composite, no visible reflection peaks were observed below 10°, indicating highly exfoliated and/or well intercalated LDH platelets within the epoxy resin [28]. However, this conjecture had to be confirmed by other technique again, such as TEM.

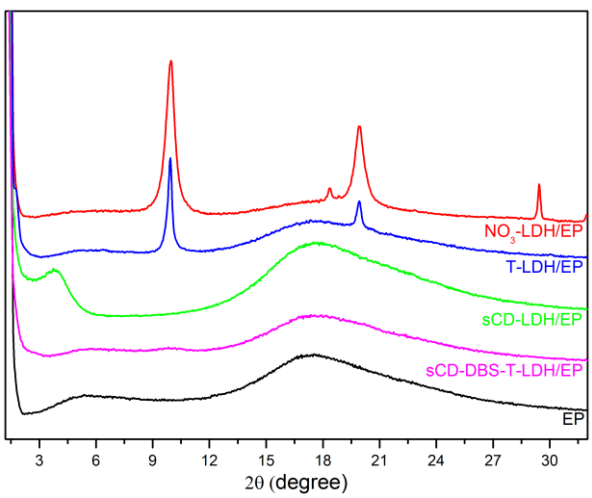

Figure 3. WAXS patterns of pure EP, NO_3-LDH/EP, T-LDH/EP, sCD-LDH/EP and sCD-DBS-T-LDH/EP composites

3.3 Transmission electron microscopy (TEM)

TEM was employed to provide more information in order to verify the results obtained from the WAXS analysis as well as to directly observe the dispersion state of LDH within the epoxy matrix. Some TEM images were shown in Fig. 4. Low and high magnification TEM images of NO_3-LDH/EP composite (Fig. 4a and 4d) showed that the large aggregates of NO_3-LDHs with the average size of >500 nm were formed. In the low magnification TEM image of T-LDH/EP composite (Fig. 4b), similar phenomenon was observed; while at the high magnification TEM image (Fig. 4e), the ordered structure of LDH was clearly observed. This was the reason why in the WAXS patterns of

NO_3-LDH/EP and T-LDH/EP, the (003) reflection peak was still observed. The dispersion state of sCD-DBS-T-LDH/EP was quite different from that of NO_3-LDH/EP and T-LDH/EP. The low magnification TEM image of sCD-DBS-T-LDH/EP (Fig. 4c) revealed a relatively better dispersion of LDH in the matrix. The high resolution image of sCD-DBS-T-LDH/EP (Fig. 4f) indicated a homogeneously disordered microstructure, which was accorded to the WAXS observations.

Transmission Electron Diffraction (TED) (Tecnai T20, FEI company) pattern was carried out by TEM in order to investigate the crystalline parameters structures of the specimens. As shown in Figure 4, for the TEM images of the NO_3-LDH/EP platelets and their selected area electron diffraction (SAED) patterns (Fig. 4 d), large number of dotes around the pointer were observed, showing existence of large poly-crystalline structures. However, in the TEM diffraction image of sCD-DBS-T-LDH/EP (Fig. 4f), there was no dote around the pointer, which represented quite small crystallites or excellent exfoliated nano- particles.

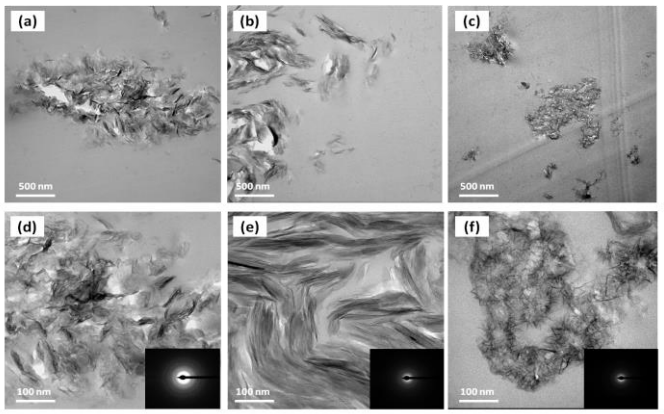

Figure 4. TEM images of NO_3-LDH/EP (a, d), T-LDH/EP (b, e) and sCD-DBS-T-LDH/EP (c, f).

3.4 Thermal Stability of epoxy nanocomposites

The thermal stability of functionalized LDH and LDH based epoxy composites had been investigated and the important results had been presented in Table 1. It found that the thermal stability of functionalized LDH had lower initial degradation temperature (T_5%) compared with that of unmodified LDH. This was caused by the introduction of organic structures in the modifiers. Moreover, the thermal stability of EP and its composites has been shown in Fig. 5. Pure EP shows a main degradation stage ranging from 380 to 500 ºC which was attributed to the decomposition of macromolecules networks. All the epoxy composites exhibited a similar one-stage degradation process. However, $T_{5\%}$ of all the epoxy composites were lowered compared to that of pure EP, indicating the introduction of LDHs caused the earlier initial decomposition of composites. The incorporation of the functionalized LDHs led to an increase in the char yield at 800 ºC. Pure EP had 14.1 % residue at 800 °C, whereas T-LDH/EP, sCD-LDH/EP and sCD-DBS-T-LDH/EP composites had 14.9%, 19.9% and 19.1% residues, respectively, at 800 °C. Notably, the experimental char residues of sCD-LDH/EP and sCD-DBS-T-LDH/EP were higher than the calculated ones, suggesting there was a synergism among the modifiers.

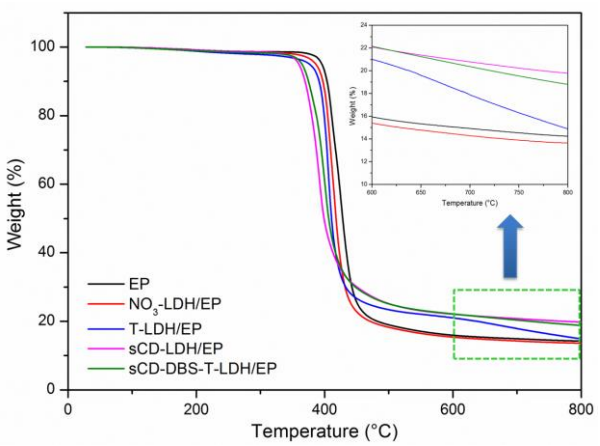

Figure 5. TGA curves of pure EP and epoxy composites under N_2 at heating rate of 10°C/min

Table 1. TGA results of LDH, organo-modified LDH and their epoxy composites

Sample	$T_{5\%}$ (°C)	T_{max} (°C)	Residue yield at 800°C (wt %)	
			Calculated	Experimental
NO_3-LDH	305	415	--	54.6
T-LDH	195	412	--	54.0
sCD -LDH	267	369	--	49.4
sCD-DBS-T-LDH	201	462	--	43.7
EP	397	425	--	14.1
NO3-LDH/EP	386	413	16.5	13.7
T-LDH/EP	376	405	16.4	14.9
sCD-LDH/EP	365	391	16.2	19.9
sCD-DBS-T-LDH/EP	358	400	15.8	19.1

3.5 Burning behaviour

The LOI values and UL-94 results of the pure epoxy and its composites were summarized in Table 3. Pure epoxy exhibited a LOI value of 23.0% and no classification in the UL-94 vertical burning test. When NO_3-LDH was added, the LOI value rise to 25.2%, but still kept no rating in the UL-94 test. Incorporating T-LDH or sCD-LDH improved the LOI value slightly, but both of them still did not pass the UL-94 V0 rating. However, it was noted that adding sCD-DBS-T-LDH into epoxy resulted in a great improvement in fire resistance and the UL-94 V0 rating was achieved in vertical burning test.

Table 2. LOI and UL94 results of EP and LDH/EP composites

Sample	LOI (%)	UL-94	Observation
Pure EP	23.0	No rating	Fire with Sooty flame
NO_3- LDH/EP	25.2	No rating	Fire with Sooty flame
T-LDH/EP	24.0	No rating	Fire with Sooty flame
sCD-LDH/EP	23.5	V-2	Fire with Sooty flame
sCD-DBS-T-LDH/EP	26.8	V-0	Extinguished immediately

Cone calorimeter tests were carried out for measuring the burning behaviours of polymeric materials in the bench-scale. Fig. 6 showed the heat release rate (HRR), total heat release (THR) and total smoke production (TSP) versus time curves of pure EP and its composites. Some important results obtained from the cone calorimeter tests, such as the time-to-ignition (TTI), char residue and the fire growth rate index (FIGRA), were summarized in Table 3. From Fig. 6a, it found that pure epoxy burnt very rapidly after ignition and the peak heat release rate value is 931 kW/m^2. Compared with pure EP, NO_3-LDH/EP and T-LDH/EP composite burnt relatively slowly and the peak HRR decreased from 931 kW/m^2 to 621 kW/m^2 and 491 kW/m^2, respectively, and the reduction in peak of HRR was 33% and 47%. However, in the case of sCD-DBS-T-LDH/EP composites the peak HRR exhibited a further decrease to 318 kW/m^2 which was corresponding to a 66% reduction of that of pure epoxy. The improved fire retardancy of sCD-DBS-T-LDH/EP was attributed to two aspects: firstly, the largest inter-layer distance of sCD-DBS-T-LDH led to the good dispersion of LDH in epoxy matrix; secondly, sCD species improved the char yield of epoxy composites during combustion.

At the end of burning, as shown in Fig. 6b pure EP had released a total heat of 81 MJ/m^2, the NO_3-LDH/EP had released almost the same amount of heat (80 MJ/m^2), whereas only 53 MJ/m^2 had been released by the sCD-DBS-T-LDH/EP nanocomposite. The significant reduction in THR meant more organic structures in the epoxy resin participated in the carbonization process and kept in the condensed phase, rather than became as "fuel" in the gas phase. This was also evidenced by the increased char residues (as listed in Table 3). With regard to the TSP, for pure EP remains the highest among all the samples. As shown in Fig. 6c, all the samples containing LDH showed relatively lower TSP compared to pure EP. The decrease in smoke formation in epoxy composites was probably due to the reduced amount of epoxy converted into organic volatiles, since the organic volatiles are the major source of smoke particles [29, 30]. The FIGRA is calculated from the ratio of PHRR and time to PHRR for all samples, as listed in Table 3. The FIGRA value of pure EP was 7.16 kW/(m^{2}s), while for NO_3-LDH/EP, T-LDH/EP, sCD-LDH/EP and sCD-DBS-T-LDH/EP they were 4.97, 2.89, 3.18 and 2.27 kW/(m^{2}s), respectively. The dramatically reduced FIGRA meant the low fire hazard of the material.

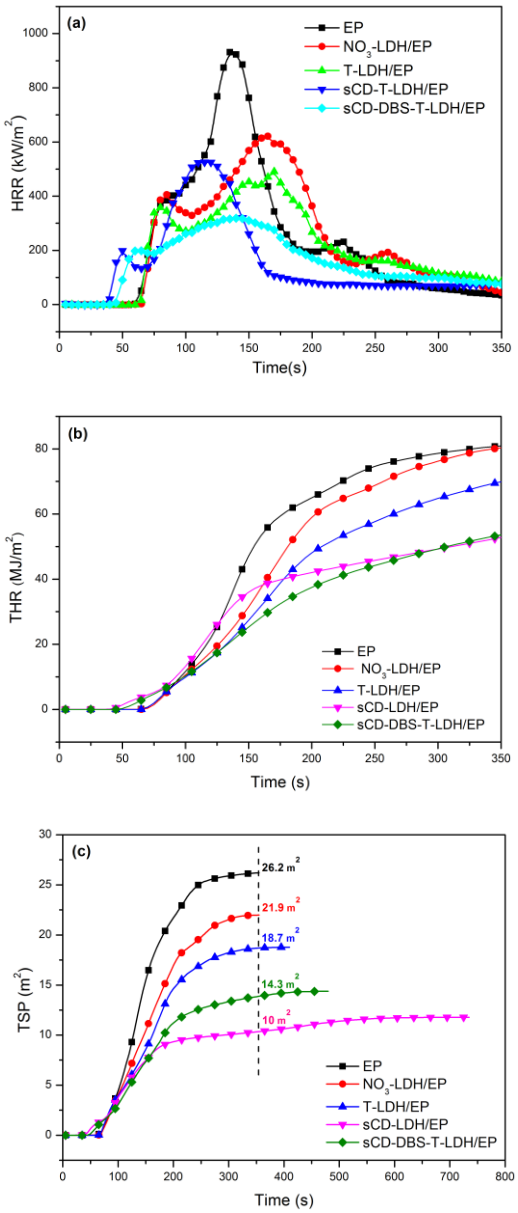

Figure 6. (a) Heat release rate, (b) total heat release and (c) total smoke production rate versus time curves of epoxy and its composites from cone calorimeter tests.

Table 3. Combustion parameters obtained from cone calorimeter.

Sample	TTI (s)	pHRR (kW/m^2)	Time to pHRR (s)	FIGRA (kW/m^{2}s)	Char residue (%)
Pure EP	58±1	931±12	130±4	7.2±0.4	14.3±0.3
NO_3-LDH/EP	65±3	621±26	125±8	4.9±0.5	21.4±1.2
T-LDH/EP	61±3	491±19	170±6	2.9±0.3	26.0±0.9
sCD-LDH/EP	37±2	525±18	165±9	3.2±0.4	24.0±1.4
sCD-DBS-T-LDH/EP	40±3	318±23	140±8	2.3±0.5	30.0±0.8

Based on the cone calorimeter results, the sCD-DBS-T-LDH/EP composite showed a significantly lower mass loss and the higher char yield compared to other samples, indicating a condensed phase mechanism for its fire resistancy. The higher char yield meant the less epoxy degraded into flammable gases, and also a thick char layer was formed on the surface of the matrix. This thick char layer served as a thermal insulating barrier that stimulated the extinguishment of the flame and prevented combustible gases from feeding the flame zone, and also separated oxygen from burning materials, as proposed in Fig. 7a. This was also accorded to the reduced heat release rate and total heat release of sCD-DBS-T-LDH/EP composite in the cone calorimeter test. To further prove this viewpoint, the morphology of samples char residues after cone calorimeter test has been investigated by SEM. As shown in Fig. 7b and 7c, the char residues of NO_3-LDH/EP showed a breaking char layer, while sCD-DBS-T-LDH/EP displayed a consolidated and thick char layer which significantly reduced heat and mass transfer and thus significantly enhanced the flame retardancy as proposed in Fig. 7a.

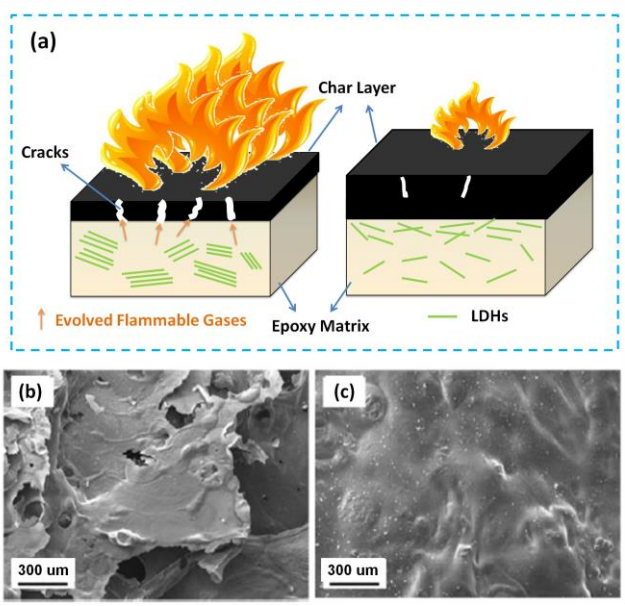

Figure 7. (a) Schematic illustration of the barrier effect of the LDH. SEM images of the residual chars of (b) NO_3-LDH/EP and (c) sCD-DBS-T-LDH/EP after cone calorimeter test.

3.6 Mechanical properties

3.6.1 Dynamic Mechanical Analysis (DMA)

The storage modulus and tan delta values of the pure epoxy and LDH-based epoxy composites were shown in Fig. 8. The storage modulus of T-LDH/EP showed the highest value among all the samples. It was attributed to the addition of taurine as modifier for LDH which enhanced the interaction between functionalized LDH and epoxy resins. In contrast, NO_3-LDH/EP showed a lower storage modulus compared to neat EP, indicating the poor interaction between the epoxy matrix and LDH layers. Glass transition temperature (T_g) was determined by the peak of tan θ curves. It was noted that the T_g of the T-LDH/EP (190 °C) was obviously lower than those of the pure EP (200 °C) and sCD-DBS-T-LDH/EP (201°C). It meant that incorporation of only taurine as modifier led to a reduction in the cross-linking density since epoxy groups were consumed to react with the NH_2- group in taurine. A reduced cross-linking density would be responsible to a decreased T_g.

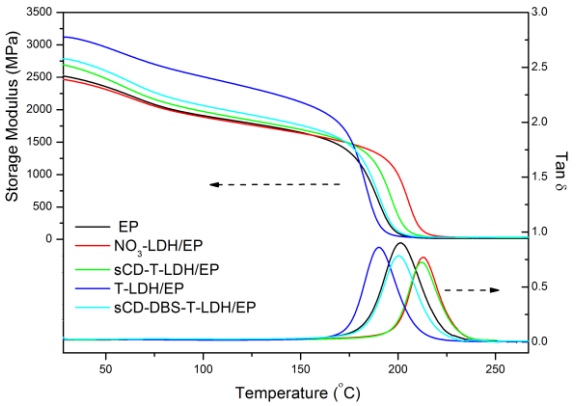

Figure 8. DMA storage modulus and tanδ versus temperature plots of epoxy and its composites.

3.6.2 Impact and Tensile properties

Impact, tensile and digital image correlation (DIC) results of pure EP and its LDH composites were presented in Fig. 9, 10 and Table 4. The results showed that the addition of NO_3-LDH or T-LDH reduced the impact strength and tensile strength of the EP composite compared with that of pure EP. As aforementioned in TEM, large agglomerations were observed for LDH in the epoxy matrix, which resulted in the poor impact strength and tensile strength. In contrast, sCD-DBS-T-LDH/EP showed much better impact and tensile strength. This was attributed to two factors: one was that the higher inter-gallery distance of sCD-DBS-T-LDH facilitated the diffusion of the epoxy chains into the inter-layers of the LDHs and thereby obtained the good dispersion of modified LDHs; the other was that the presence of taurine as the modifier that improved the interaction between epoxy matrix and LDH layers.

During tensile test, digital image correlation (DIC) technique had been conducted to capture the state of strain distribution on the samples. The state of strain distribution for sCD-DBS-T-LDH/EP and NO_3-LDH/EP had been represented in Fig.10. sCD-DBS-T-LDH/EP had higher homogeneity in strain distribution, while the poor distribution of strain was observed in NO_3-LDH/EP. Based on this result, more homogenous distribution of starin field in sCD-BDBS-T-LDH/EP resulted in higher mechanical properties.

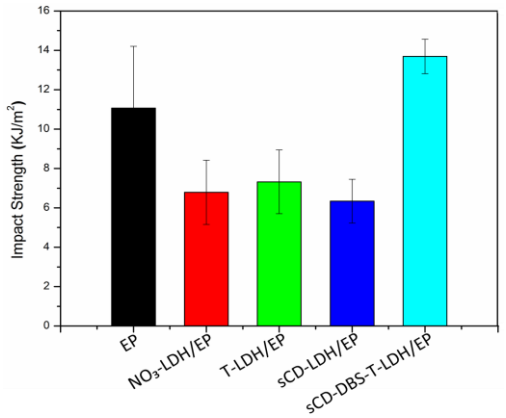

Figure 9. Impact behaviour of pure EP and epoxy composites

Table 4. Tensile results

Sample	Tensile strength at break (MPa)	Young modulus (GPa)	Elongation at break (%)
EP	56.4±8.6	3.2±0.1	4.2±0.1
NO_3-LDH/EP	36.7±2.7	3.6±0.2	4.0±0.2
T-LDH/EP	42.1±2.8	2.6±0.1	3.4±0.2
sCD-LDH/EP	40.0±3.0	3.7±0.1	2.6±0.2
sCD-DBS-T-LDH/EP	51.5±2.5	3.3±0.1	4.8±0.1

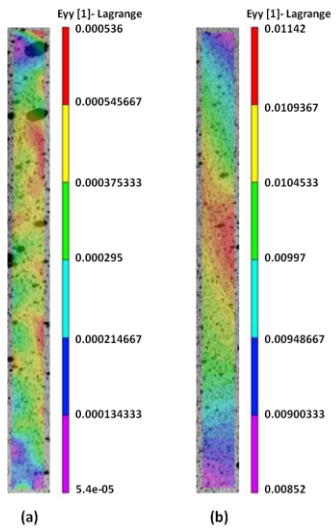

Figure 10. Digital image correlations of NO3-LDH/EP (a) and sCD-DBS-T-LDH/EP (b)

4. Conclusions

In this work, multi-modifiers' system for preparing functionalized LDHs and these LDHs based epoxy composites had been developed by sophisticatedly utilizing hydroxypropyl-sulfobutyl-beta-cyclodextrin sodium (sCD) sodium dodecylbenzenesulfonate (DBS) and taurine (T) as functional modifiers. TEM and WAXS results revealed that sCD-DBS-T-LDH/EP showed better dispersion state than other epoxy composites containing un-modified LDH and/or other functionalized LDH. A UL-94 V0 rating flame retardant material was achieved for epoxy composite with 6 wt% of sCD-DBS-T-LDH. The cone calorimeter results showed that the addition of sCD-DBS-T-LDH significantly reduced the HRR, THR, FIGRA and improved the char residue after fire test, compared with those of other samples, indicating that sCD-DBS-T-LDH was a high efficient nano fire retardant for epoxy.. This improved fire retardancy was contributed to the efficient char protection layer formed during the burning which effectively inhibited the heat and mass transfer and generated low organic degradation volatiles into gas phase. Also, sCD-DBS-T-LDH/EP exhibited the improved impact and tensile properties compared with its counterparts due to the good dispersion state of LDH and the strong interaction between epoxy matrix and LDHs. This multi-modifiers' system developed in this paper has been offering a promising solution for developing multifunctional high performance fire retardant polymer nanocomposite.

Acknowledgements

This research is partly funded by the European Commission under the 7th Framework Programme (Marie Curie Career Integration Grant), European Project COST Action MP1105 "FLARETEX" and Ramón y Cajal grant (RYC-2012-10737). Also, the authors are grateful to the nice discussion and comments from Mr.Mohammad Marvi-Mashhadi in IMDEA Materials Institute.

Notes and references

[a] Madrid Institute for Advanced Studies of Materials (IMDEA Materials Institute), C/Eric Kandel, 2, 28906 Getafe, Madrid, Spain

† Corresponding Author:
De-Yi Wang; E-mail: deyi.wang@imdea.org

1 X. Wang, Y. Hu, L. Song, W. Y. Xing, H. D. Lu, P. Lv, G. X. Jie, Polymer 2010, 51, 2435-2445.

2 Z.K. Chen, G. Yang, J.P. Yang, S.Y. Fu, L. Ye, Y.G. Huang. Polymer 2009, 50, 1316-1323.

3 M. Morell, X. Ramis, F. Ferrando, Y.F. Yu, A. Serra. Polymer 2009, 50, 5374-5383.

4 X. Wang, L. Song, W. Y. Xing, H. D. Lu, Y. Hu, Materials Chemistry and Physics 2011, 125, 536-541.

5 B. K. Kandola, A. R. Horrocks, P. Myler, D. Blair, J. Applied Polymer Science. 2003, 88, 2511–2521.

6 X. Wang, Y. Hu, L. Song, W. Y. Xing, H. D. Lu, Polymers for Advanced Technologies 2012, 23, 190-197.

7 C.H. Lin, T.Y. Hwang, Y.R. Taso, T.L. Lin. Macromolecule Chemistry Physics 2007, 208, 2628-2641.

8 X. Wang, Y. Hu, L. Song, W. Y. Xing, H. D. Lu, P. Lv, G. X. Jie, Polymers for Advanced Technologies 2011, 22, 2480-2487.

9 Y. Zheng, K. Chonung, X.L. Jin, P. Wei, P.K. Jiang. Journal of Applied Polymer Science 2008; 107, 3127-3136.

10 L.A. Mercado, M. Galia, J.A. Reina. Polymer degradation and Stability 2006, 91, 2588-2594.

11 X. Wang, Y. Hu, L .Song, W.Y. Xing, H. D. Lu, Journal of Polymer Science Part B-Polymer Physics 2010, 48, 693-705.

12 H.Y. Yang, X. Wang, B. Yu, L. Song, Y. Hu, R. K. K. Yuen, Thermochimica Acta, 2012, 535, 71-78.

13 C. Li, J.T. Wan, E. Kalali, H.Fan, D.Y. Wang. Journal of Materials Chemistry A, 2014, DOI: 10.1039/C4TA05740F

14. J.H. Zhang, S.D. Juan, E. Cubillo, J. Santarén, D.Y. Wang. Chinese Journal of Chemistry, 2015, DOI: 10.1002/cjoc.201400828

15 D. Y. Wang, A. Das, F. R. Costa, A. Leuteritz, Y. Z.Wang, U. Wagenknecht, G. Heinrich, Langmuir 2010, 26, 14162-14169.

16 W. Chen, B. Qu, Chemistry of Materials, 2003, 15, 3208−3213.

17 M. Darder, L. B. Mar, P. Aranda, F. Leroux, R. H. Eduardo, Chemistry of Materials, 2005, 17, 1969-1977.

18 X. Wang, S. Zhou, , W. Y. Xing, B. Yu, X. M. Feng, L. Song, Y. Hu, Journal of Materials Chemistry A 2013, 1, 4383–4390.

19 N.J. Kang, D.Y. Wang, B. Kutlu, P.C Zhao, A. Leuteritz , U. Wagenknecht, G. Heinrich . ACS Applied Materials & Interfaces 2013, 5, 8991−8997.

20 D. Y. Wang, A. Das, A. Leuteritz, R. N. Mahaling, D. Jehnichen, U. Wagenknecht,; G. Heinrich, RSC Advances. 2012, 2, 3927-3933.

21 N. Nhlapo, T. Motumi, E. Landman, S. M. C. Verryn, W. W. J. Focke, Journal of Material Science, 2008, 43, 1033-1043.

22 N. Iyi, Y. Ebina, T. J. Sasaki, Journal of Materials Chemistry 2011, 21, 8085-8095.

23 E. M. Moujahid, J. P. Besse, F. J. Leroux, Journal of Materials Chemistry 2003, 13, 258-264.

24 J. H .Choy, S. Y. Kwak, J. S. Park, Y. J. Jeong, J. J. Portier, Journal of the American Chemical Society,1999, 121, 1399-1400.

25 M. A. Woo, T. W. Kim, M. J. Paek, H. W. Ha, J. H. Choy, S. J. J. Hwang, Journal of Solid State Chemistry 2011, 184, 171-176.

26 N.J. Kang, D.Y. Wang. Journal of Materials Chemistry A 2013, 1, 11376 -11383.

27.R. Yong, M. Xueqin, Y. Shuqin, S. Xiaodong, US8278437 B2

28 C. Katsoulis, E. Kandare, B.K. Kandola. Polymer Degradation and Stability 2011, 96, 529-540.

29 Y.Y. Dong, Z. Gui, Y. Hu, Y. Wu, S.H. Jiang. Journal of Hazardous Materials 2012, 209, 34-39.

30 X. Wang, W.Y. Xing, X.M. Feng, B. Yu, H.D. Lu, L. Song, Y. Hu. Chemical Engineering Journal 2014, 250: 214-221.